

# Dielectric and ferroelectric properties of Nb-doped Ba<sub>0.8</sub>Sr<sub>0.2</sub>TiO<sub>3</sub> ceramics

L. Yang · W. Q. Cao

Published online: 4 May 2007  
© Springer Science + Business Media, LLC 2007

**Abstract** Ferroelectric and dielectric properties were investigated for Ba<sub>0.8</sub>Sr<sub>0.2</sub>Ti<sub>(1-5/4x)</sub>Nb<sub>x</sub>O<sub>3</sub> ceramics with different Nb<sub>2</sub>O<sub>5</sub> concentrations. The relations between the ceramic structures and those properties were discussed. The Ba<sub>0.8</sub>Sr<sub>0.2</sub>TiO<sub>3</sub> doping with 0.01 mol% Nb<sub>2</sub>O<sub>5</sub> appears to have a strong ferroelectric effect and better dielectric properties. The max permittivity ( $\epsilon_{\max}$ ) is up to 7,521.3 and Ba<sub>0.8</sub>Sr<sub>0.2</sub>Ti<sub>(1-5/4x)</sub>Nb<sub>x</sub>O<sub>3</sub> ceramics has higher permittivity even at room temperature. The permittivity presents broadened curves at large temperature ranges, which suggests a non Curie–Weiss behavior near the transition temperature. The diffuse phase transition coefficient ( $\delta$ ) for Ba<sub>0.8</sub>Sr<sub>0.2</sub>Ti<sub>(1-5/4x)</sub>Nb<sub>x</sub>O<sub>3</sub> doping with 0.01 mol% Nb<sub>2</sub>O<sub>5</sub> reaches 0.098, and its  $P$ – $E$  loop expresses a diffusing curve. The remanent polarization ( $2P_r$ ) and coercive field are 31.3  $\mu\text{C}/\text{cm}^2$  and 10 kV/cm, respectively. The  $P$ – $E$  loop presents a diffusing curve, which is relative to the relaxor characteristic.

**Keywords** Ferroelectric ceramics · Dielectric · Diffuse phase transition · Ba<sub>0.8</sub>Sr<sub>0.2</sub>Ti<sub>(1-5/4x)</sub>Nb<sub>x</sub>O<sub>3</sub>

## 1 Introduction

Barium strontium titanate, Ba<sub>x</sub>Sr<sub>1-x</sub>TiO<sub>3</sub> (BST), has excellent ferroelectric and dielectric properties, which has attracted much attention. It was widely used in devices

such as capacitors, phase shifting in antenna and radar equipment, ferroelectric memory for computers, etc. [1, 2]. Doping of Ba<sub>x</sub>Sr<sub>1-x</sub>TiO<sub>3</sub> to fine tune its properties for particular applications is therefore an interesting research task. Doping of the Ba<sub>x</sub>Sr<sub>1-x</sub>TiO<sub>3</sub> ( $x=0.6$  and 0.7) compositions with different elements are being widely investigated [3–7] due to its high dielectric permittivity, small dielectric loss, and transition temperatures near the room temperature of the undoped system. Regarding the rise of the devices' working temperature, the present work is dedicated to the study of stabilities in high dielectric constant, ferroelectric properties, and relation between ferroelectric properties and the structure around the room temperature for the Nb-doped Ba<sub>0.8</sub>Sr<sub>0.2</sub>TiO<sub>3</sub> ceramics.

## 2 Experiments

Due to the similar electronegativity and the ionic radii for both Nb<sup>5+</sup> and Ti<sup>4+</sup>, the compositions of the samples studied are given by Ba<sub>0.8</sub>Sr<sub>0.2</sub>Ti<sub>(1-5/4x)</sub>Nb<sub>x</sub>O<sub>3</sub> (BST20), where  $x=0.01$ , 0.05, and 0.1. Ceramic samples were prepared by the conventional solid-state reaction technique using materials of BaCO<sub>3</sub>, SrCO<sub>3</sub>, TiO<sub>2</sub>, and Nb<sub>2</sub>O<sub>5</sub>. The raw materials were calcined at 1100 °C for 2 h. The calcined mixture was ball-milled and pressed into pellet disks (10 mm in diameter, 1 mm in thickness). The samples were sintered at 1280 °C for 4 h. The crystal phase composition was studied by X-ray diffraction (XRD). The PHILIPS PW-1710 with CuK $\alpha$  anode ( $\lambda=1.5406 \text{ \AA}$ ) was used for XRD. The 10-kV JEOL microscope model M5400 was used for analyzing the microstructure of the samples. The HP4294 was used to test the dielectric properties. The hysteresis meter (RT-6000HVS) was used to measure the  $P$ – $E$  hysteresis loop.

L. Yang · W. Q. Cao (✉)  
School of Physics and Electronic Engineering, Hubei University,  
Wuhan 430062, China  
e-mail: caowang62@yahoo.com.cn

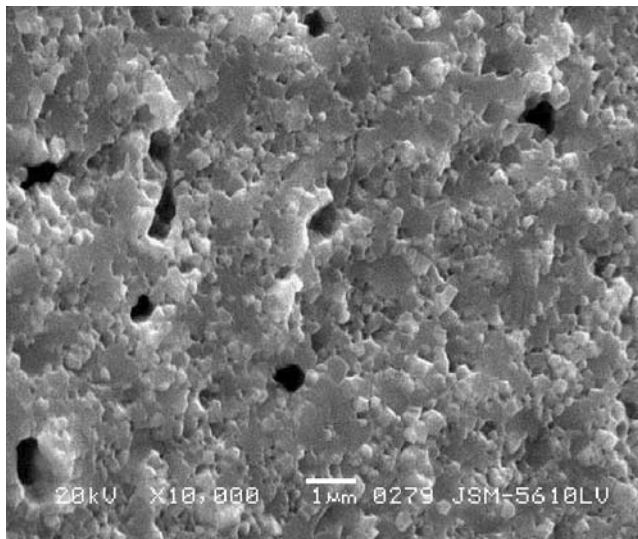


**Fig. 1** The SEM of BST20 doping with 0.1mol% Nb

### 3 Results and discussion

Figure 1 shows the SEM micrographs of the  $\text{Ba}_{0.8}\text{Sr}_{0.2}\text{Ti}_{(1-5/4x)}\text{Nb}_x\text{O}_3$  ( $x=0.01$ ). The crystal grains grow well and connected with each other tightly, and little air vents can also be seen in the ceramics.

Figure 2 exhibits the XRD patterns of the  $\text{Ba}_{0.8}\text{Sr}_{0.2}\text{Ti}_{(1-5/4x)}\text{Nb}_x\text{O}_3$  ( $x=0, 0.01, 0.05$ , and  $0.1$ ). Compared with the standard XRD pattern of the  $\text{Ba}_{0.7}\text{Sr}_{0.3}\text{TiO}_3$ , the samples have perfect perovskite phase. The crystal parameters grow a little large with the increase of Nb concentration (Table 1), which can be considered as a result from the substitution of larger  $\text{Nb}^{5+}$  for small  $\text{Ti}^{4+}$ .

The dependences of the dielectric constant and the dielectric loss on temperature measured at 1 kHz for all the studied compositions are shown in Figs. 3 and 4,

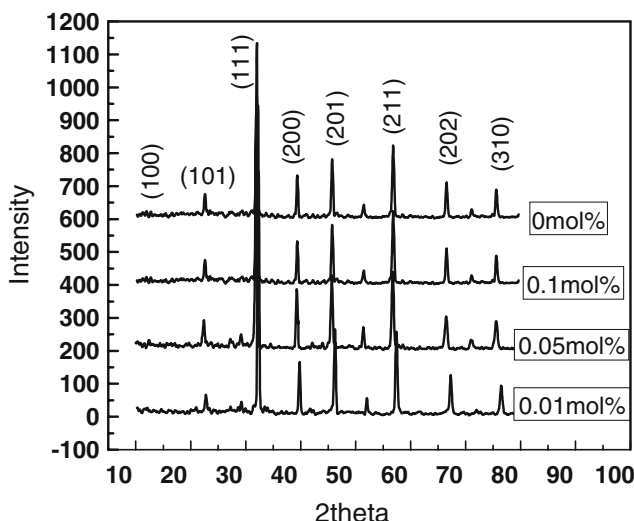


**Fig. 2** XRD pattern of BST20 ceramics system

**Table 1** Lattice parameters for BST20 of all composition.

Composition	a or b (Å)	c (Å)	V (Å <sup>3</sup> )
0	3.980	3.981	63.06063
0.01	3.982	3.983	63.15574
0.05	3.993	3.9998	63.77301
0.1	4.038	4.042	65.9066

respectively. The dielectric constant curve of BST20 ceramic system doping with 0.01mol% Nb presents a broadened peak, which suggest a non Curie–Weiss behavior near the transition temperature.

Figure 5 shows an explicit frequency dispersive relation of the dielectric constant. The phase transition temperature is 56 °C. There are little differences among curves at lower temperature part of the peaks, but larger differences at higher temperature part of the peaks. Therefore, the frequency dispersive property can be described with a diffuse phase transition relation, i.e., the diffuse phase transition coefficient ( $\delta$ ) determined by the developed Smolenskii's relation [3, 8]:

$$\frac{1}{\varepsilon} - \frac{1}{\varepsilon_{\max}} = C(T - T_m)^{\gamma} \quad (1)$$

where

$$C = \frac{1}{2\varepsilon_{\max}} \delta^2 \quad (2)$$

Obviously, the transformed experiment results demonstrate a linear relation with the transformed temperature in Fig. 6. So a fitting relation of  $(\frac{1}{\varepsilon} - \frac{1}{\varepsilon_{\max}})$  to  $\log(T - T_m)$  is accordant with the experiments shown in Fig. 6 with the following expression:

$$\log\left(\frac{1}{\varepsilon} - \frac{1}{\varepsilon_{\max}}\right) = -6.2 + 1.6 \log(T - T_{\max}) \quad (3)$$

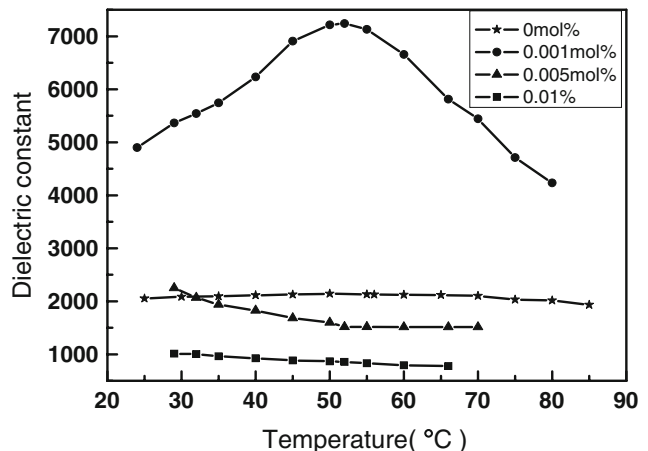


**Fig. 3** Dependence of the dielectric constant with temperature

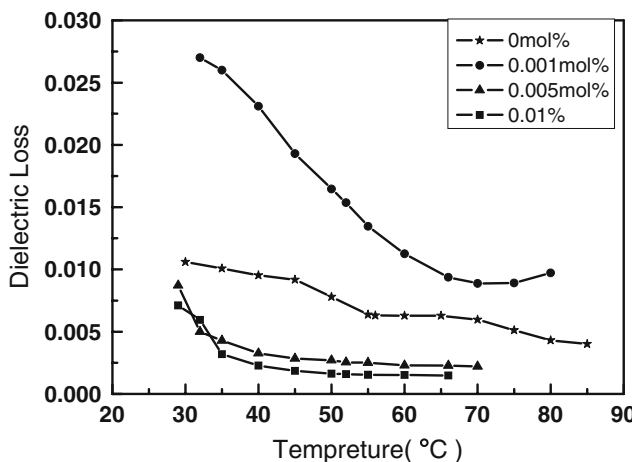


**Fig. 4** Dependence of the dielectric loss with temperature

The data in Eq. 2 means that the diffuse phase transition coefficient ( $\delta$ ) is 0.098, and the factor  $\gamma$  is 1.6.

Figure 7 shows the  $P$ - $E$  hysteresis loop of the BST20 at room temperature. Figure 7a shows that the  $2P_r$  is  $31.3 \mu\text{C}/\text{cm}^2$  and the  $E_c$  is  $10 \text{ kV}/\text{cm}$  for BST doping with 0.01mol% Nb. The  $P_r$  and  $E_c$  increased with the drive voltage. When the voltage increased, the polarization does not grow to the saturated line as usual, but increasing and then decreasing. There were many order and disorder microregions in the ceramics, and some regions' polaron have frozen. When the voltage increased, these polarons are stimulated and result in the polarization–voltage line diffusion such as the  $P$ - $E$  hysteresis loop showed in Fig. 7(a). Figure 7(b) shows the  $P$ - $E$  hysteresis loop in a different composition. It can be observed that the BST20 ceramic system doping with 0.01mol% Nb has the best ferroelectric properties.

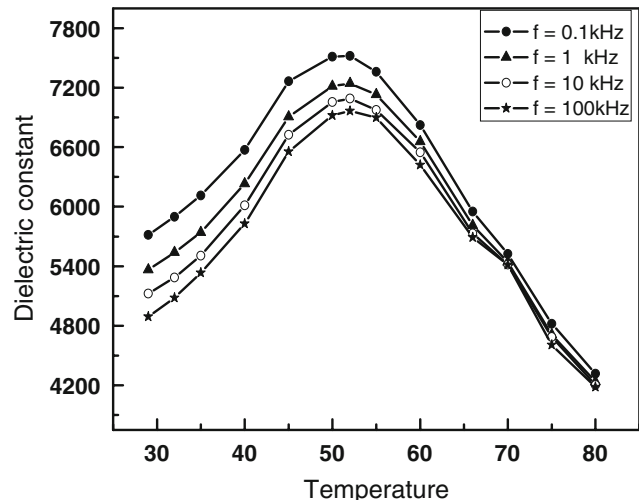


**Fig. 6** Dependence of  $\log(1/\epsilon - 1/\epsilon_{\max})$  with the  $\log(T - T_{\max})$  for the BST20 ceramic system doping with 0.01mol% Nb. Square points are experiment results and the line is the Smolenskii's relation

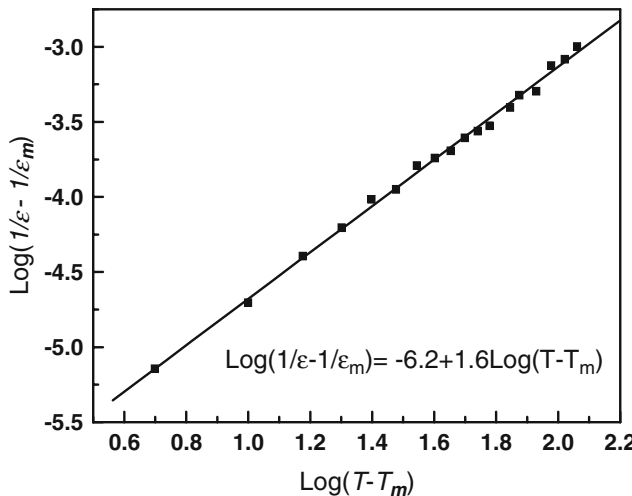
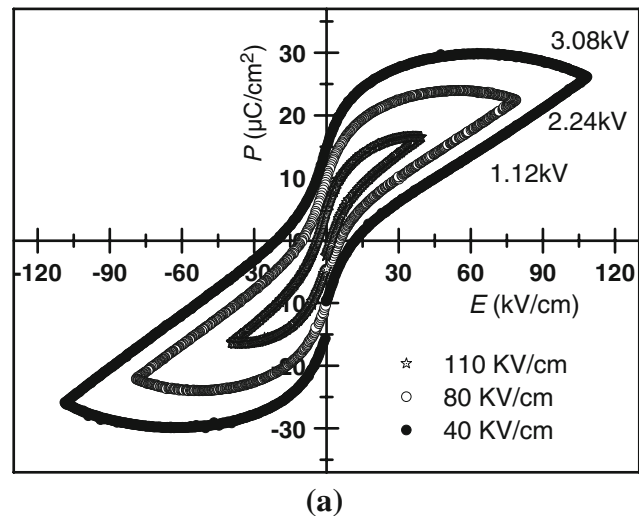
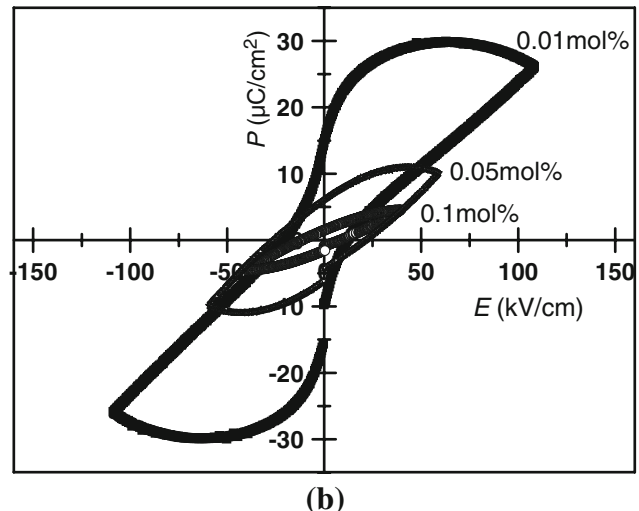


**Fig. 5** Dependence of the dielectric constant with temperature for  $x=0.01$  at different frequency



(a)



(b)

**Fig. 7** (a)  $P$ - $E$  hysteresis loop of a different voltage of BST20 doping with 0.01mol% Nb. (b)  $P$ - $E$  hysteresis loop of different composition

#### 4 Conclusion

The  $\text{Ba}_{0.8}\text{Sr}_{0.2}\text{Ti}_{(1-5/4x)}\text{Nb}_x\text{O}_3$  ( $x=0.01$ ,  $0.05$ , and  $0.1$ ) system ceramic was sintered at  $1280^\circ\text{C}$  for  $4\text{ h}$ . The  $\text{Ba}_{0.8}\text{Sr}_{0.2}\text{TiO}_3$  doping with  $0.01\text{ mol\% Nb}_2\text{O}_5$  has strong ferroelectric and good dielectric properties. The max permittivity ( $\epsilon_{\max}$ ) is  $7,521.3$  and the permittivity at room temperature remains at high value. The relation of permittivity with temperature for  $\text{Ba}_{0.8}\text{Sr}_{0.2}\text{TiO}_3$  doping with  $0.01\text{ mol\% Nb}_2\text{O}_5$  presents broadened curves, which suggest a non Curie–Weiss behavior near the transition temperature near the room temperature, but follows the developed Smolenskii's relation,  $\frac{1}{\epsilon} - \frac{1}{\epsilon_{\max}} = C(T - T_m)^\gamma$ , where  $C$  is  $10^{-6.2}$  and  $\gamma$  is  $1.6$ . The diffuse phase transition coefficient ( $\delta$ ) of BST system doping with  $0.01\text{ mol\% Nb}_2\text{O}_5$  was  $0.098$ . The BST20 system ceramic performs an explicit frequency dispersive relation or a relaxor characteristic. The remanent polarization ( $2P_r$ ) and coercive field are  $31.3\text{ }\mu\text{C/cm}^2$  and  $10\text{ kV/cm}$ , respectively, for  $\text{Ba}_{0.8}\text{Sr}_{0.2}\text{TiO}_3$  doping with  $0.01\text{ mol\% Nb}_2\text{O}_5$ . And the  $P$ – $E$  loop presents a diffusing curve, which is relative to the relaxor characteristic.

**Acknowledgments** This paper is sponsored by the Innovation Team Foundation of Hubei Province, China; Excellent Creative Research Team Project of Hubei Province; and the Key Project of Hubei University. The authors thank professor Brahim Elouadi for his helpful reviews.

#### References

1. L. Zhang, W.L. Zhong, G. Wang, Solid State Commun. **10**(12), 761 (1998)
2. S. Zafar, P. Chu, T. Remmel, R.E. Jones, B. White, D. Gentile, B. Jiang, B. Melnick, D. Taylor, P. Zucher, S. Gillespie, Mater. Res. Soc. Symp. Proc. **43**, 15 (1998)
3. S. Garcia, R. Font, J. Portelles, R.J. Quinones, J. Heiras, J.M. Siqueiros, J. Electroceram. **6**(2), 101 (2001)
4. S.B. Herner, F.A. Selmi, V.V. Varandan, V.K. Varandan, Mater. Lett. **15**, 317 (1993)
5. T. Ishiya, S. Tashiro, H. Igarashi, Jpn. J. Appl. Phys. **34**, 5309 (1995)
6. T. Yamamoto, S. Takao, Jpn. J. Appl. Phys. **31**, 3120 (1992)
7. D. Kolar, M. Trontell, Z. Stadler, J. Am. Ceram. Soc. **65**, 10 (1982)
8. G.A. Smolenskii, V.A. Isupov, A.I. Agranovskaya, Sov. Phys. Solid State **2**(11), 2584 (1960)